Experimental and numerical investigations of the heating influence on the Ti5553 titanium alloy machinability

Vincent Wagner, Mahmoud Harzallah, Maher Baili, Gilles Dessein, Daniel Lallement

▶ **To cite this version:**

Vincent Wagner, Mahmoud Harzallah, Maher Baili, Gilles Dessein, Daniel Lallement. Experimental and numerical investigations of the heating influence on the Ti5553 titanium alloy machinability. Journal of Manufacturing Processes, 2020, 58, pp.606-614. 10.1016/j.jmapro.2020.08.018 . hal-03631262

HAL Id: hal-03631262
https://hal.science/hal-03631262

Submitted on 5 Apr 2022

HAL is a multi-disciplinary open access archive for the deposit and dissemination of scientific research documents, whether they are published or not. The documents may come from teaching and research institutions in France or abroad, or from public or private research centers.

L'archive ouverte pluridisciplinaire **HAL**, est destinée au dépôt et à la diffusion de documents scientifiques de niveau recherche, publiés ou non, émanant des établissements d'enseignement et de recherche français ou étrangers, des laboratoires publics ou privés.

OATAO

Open Archive Toulouse Archive Ouverte

OATAO is an open access repository that collects the work of Toulouse researchers and makes it freely available over the web where possible

This is an author's version published in: http://oatao.univ-toulouse.fr/28924

Official URL:
https://doi.org/10.1016/j.jmapro.2020.08.018

To cite this version:

Wagner, Vincent and Harzallah, Mahmoud and Baili, Maher and Dessein, Gilles and Lallement, Daniel *Experimental and numerical investigations of the heating influence on the Ti5553 titanium alloy machinability.* (2020) Journal of Manufacturing Processes, 58. 606-614. ISSN 15266125

Any correspondence concerning this service should be sent to the repository administrator: tech-oatao@listes-diff.inp-toulouse.fr

Experimental and numerical investigations of the heating influence on the Ti5553 titanium alloy machinability

V. Wagner[a,*], M. Harzallah[a], M. Baili[a], G. Dessein[a], D. Lallement[b]

[a] Laboratoire Génie de Production (LGP), Université de Toulouse, INP-ENIT, Tarbes, France
[b] Safran Landing System, Etablissement de Bidos, 64401 Oloron Sainte Marie, France

Keywords:
Hot machining
Ti5553 titanium alloy
Tool wear
Chip formation
Microstructure analysis

A B S T R A C T

The use of titanium alloys has become more widespread in recent years. Regardless, although research work is enhancing, productivity levels remain low. Several alternatives have been considered and one of the techniques is envisaged is heating assistance. The objective is then to increase the temperature locally in order to benefit from thermal softening. However, the research is based on power-controlled laser assistance where the temperature levels are not considered. For this purpose, this article suggests a study based on a new experimental device which allows to control the temperature of the machined part. After presenting the device and the material used (Ti5553), the study first shows the effect of temperature on cutting forces. Three temperature ranges and three trends are shown. A first where temperature has no effect, a second when there is a substantial gain and a third where temperature has a real impact. In order to understand the existing links, two methods were used. A finite element model integrating a new law of behaviour was developed and shows the very high temperature levels reached in the cutting areas. Then, to better understand the phenomena governing cutting, we looked at chip formation and the link between chip formation, temperature and its effect on the microstructure. After all, an economic analysis completes this article and highlights the small gains of this assistance.

1. Introduction

Ti5553 titanium alloy is increasingly used and its machining stays always a problematic. In fact, its low thermal conductivity combined with its microstructure and its high mechanical properties make it a low machinability alloy [1]. Recently, several studies have been conducted to investigate the Ti5553 machinability and thus, to enhance the productivity, the tool life and the surface integrity. Since the limitations of Ti5553 conventional machining (without assist), several assistance techniques have been applied to achieve these goals. These techniques can be sorted into two groups. The first group intended to cool the workpiece to decrease the temperature at the tool/workpiece interface [2,3]. employed the high-pressure water jet assistance during Ti-6Al-4 V titanium alloy machining. They found an increase of about 300 % in tool life compared to dry machining. Using the same technologie [4], registered an increase of 185 % on the tool life when machining the Ti555-3 alloy. The cryogenic assistance is also widely used in machining and, especially for titanium alloy. Most cryogenic machining studies have shown improved machinability when freezing the workpiece or cooling the tool using a cryogenic coolant [2]. The second group focused on heating of the workpiece to decrease its mechanical properties. Hot machining has received the attention of researchers in the metal cutting domain and a few research was carried out during the recent years [5]. employed the Laser-assisted technique (LAM) during machining of Ti-6Al-4 V titanium alloy. The authors noted a high reduction of cutting force which can exceed the 50 %. An economic analysis is carried out by [6] during the Inconel 718 machining. They demonstrated that the LAM technique can provide a strong reduction in cutting forces, a strong improvement in surface roughness (2 at 3 times) and a 200–300 % increase of tool life of ceramic tools over conventional machining. However, to make thermally assisted machining more attractive some attempts use a localised heat sources such as plasma and laser. Although laser assistance could increase the machinability of hard-to-cut materials, but it presents some disadvantages like the efficiency, the high-power consumption, the human security and the high cost. Indeed, many researchers used conventional heat sources such as furnaces, torches or induction technique for the workpiece heating [7] and more recently [8]. By means of gas flame heat machining technique [9] analyse the effect of the machining parameters on the surface integrity, the cutting forces and the tool life. They show an improvement on the surface finish and a decrease on the cutting forces.

It was observed a decrease of 33.95 % flank wear compared to

* Corresponding author.
E-mail address: vincent.wagner@enit.fr (V. Wagner).

conventional machining. [10] employed a dedicated induction system for hot turning. The system is based on an improved induction coil which is adapted to heat a localised portion of the machined part. Using the same technique [11] investigated the tool life improvement in milling of Titanium Alloy Ti-6Al-4 V through workpiece preheating. The authors concluded that with preheating at 650 °C it is possible to increase the tool life by 2.7 times compared to the experiment tests made at room temperature.

The aim of this study is to improve the machinability of the Ti5553 titanium alloy with the assistance of high frequency induction heating. Experimental and numerical investigations is carried out at various preheating temperatures. The paper presents firstly, the developed experimental set-up that used for workpiece preheating. Then, the experimental tests are described and the influence of the hot machining on the cutting forces as well as the chip morphology is discussed. By means of 3D FE orthogonal cutting model, the chip formation process is simulated and compared to experimental observations. Moreover, a discussion is made regarding the hot machining influence on the chip morphology and the material microstructure. After all, the economic benefits and limits of this assistance is discussed.

2. Experimental set-up

For the workpiece heating, a high frequency induction system has been used and adapted to the turning operation. The heating device is defined by a semicircular inductor which envelops the piece.

The part is divided in two with a first mounted in the machine mandrill and a second to be machined. This is fixed in a specific rotating component which is designed to integrate thermocouples. The temperature of the workpiece is controlled by a thermal camera and 4 thermocouples positioned as described in Fig. 1. It should be noticed, the signal recoveries from thermocouples are carried through a rotating collector which is fixed on the chuck of the lathe.

Fig. 2 exhibits the temperature evolution during a test in regarding the thermocouples T2 and T3 positioned differently. T2 is close to the radial depth and to the part extremity contrary to T3 which is deeper radially and axially. The temperature shown in the next section is an average between the thermocouple's and the IR camera's measures.

The preheating cycle is based in two phases. The first consists of the workpiece heating during its rotation until achieving the preselected temperature. During this phase, the part turns to get a homogeneous temperature. At the end of the first phase where the temperature desired is partially obtained, the part rotation is stopped for moving the tool and prepare the measure device. The inductor is also shut down to avoid the heating of only one section of the part. Although the experimental set-up is operational, the rotation and the heating start until to get the desired temperature. Once the temperature is reached, a 15 mm turning operation is performed.

2.1. Material of study

All tests were performed on titanium alloys Ti5553. The chemical composition is Aluminum 5 %, Molybdenum 5 %, Vanadium 5 % and Chromium 3 %. This alloys is a beta-metastable structure and it is a part of the near-beta-alloys family of titanium. The titanium used in this work is firstly heat-treated and after forged. The heat treatment is divided into three parts :

1 heating to 800 °C during 4 h,
2 free cooling,
3 aging at 600 °C for 8 h

The resulting microstructure is shown Fig. 3. The difference between the two phases of titanium can be observed in using a spectral analysis technic. The lowest concentration of aluminium is found in the α phase. During the heat treatment, a combination of the α and β phases results in some nodules $\alpha_{p,}$ which coalesce during the tempering. This last treatment also generates fine α_s precipitates in the β matrix. As shown in this figure, the size of the beta phase is large ($\varphi = 500\,\mu m$). EBSD (Electron Backscatters Diffraction) analysis correlates with observations made by [12].

2.2. Cutting conditions

The cutting speed (Vc = 35 m/min), the feed is (0,1 m/rev), the radial depth (ap = 3 mm) are steady. This cutting speed was chosen according to the Tool Material Pair methodology but made at room temperature [13]. The insert used is CNMG 160612 - QM1105 (rake angle = 13°, backing edge of 0.12 mm at 13° combined with a honing of 0.02 mm).

3. Experimental results

3.1. Cutting forces

Fig. 4 exhibits the evolution of the cutting forces according to the temperature of the workpiece. Four values occur : Fc, Ft, Fa and R which are respectively the component co-linear to the cutting speed, to the feed and to the cutting edge. After all, R is the cutting force resultant. The decrease in the percentage according to the initial value is shown on the graph with the blue dot line. The evolution of cutting forces describes three tendencies according to temperature ranges. The first one is between the room temperature and 100 °C. No noticeable effect on the heating of the measured forces were detected. All

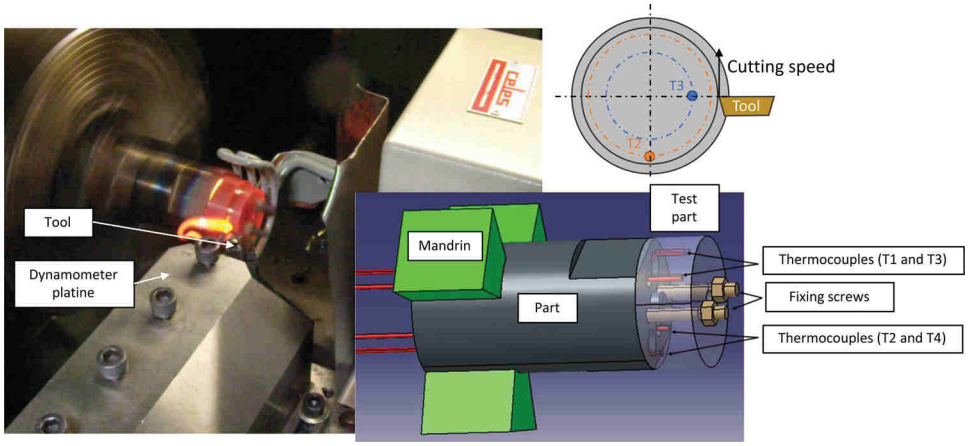

Fig. 1. Experimental set-up description.

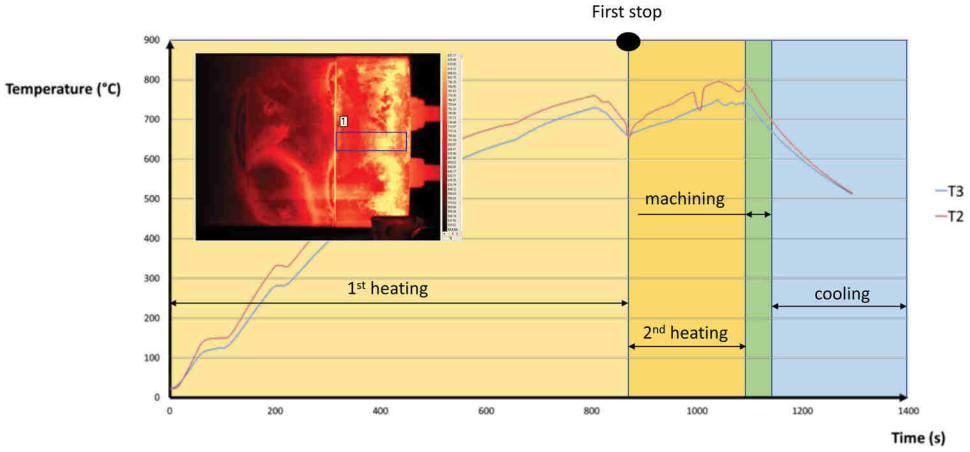

Fig. 2. Experimental heating of workpiece material.

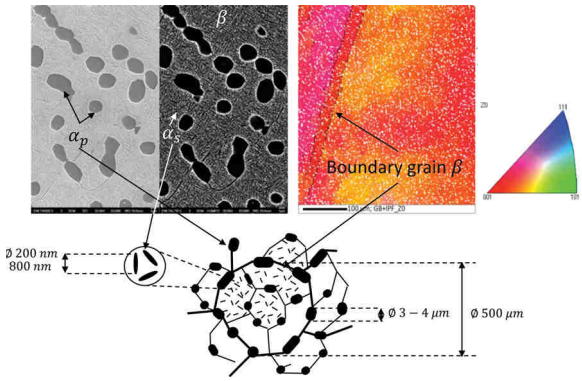

Fig. 3. Ti5553 original microstructure.

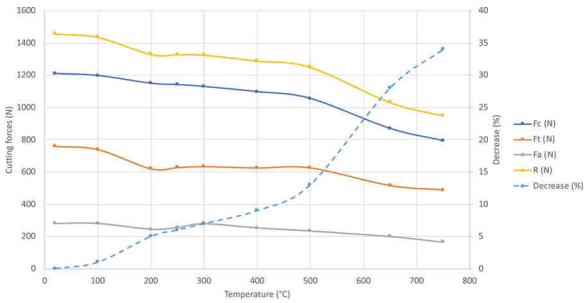

Fig. 4. Cutting forces evolution with temperature.

components are consistent. The second tendency is between 100 °C and 500 °C. A slight decrease of the forces is observed. The last section is defined for the temperatures higher than 500 °C where a considerable drop of forces was observed. Concerning each component, their evolution are identical. A larger decrease occurs for the Ft components when the temperature is 200 °C. An increase of 750 °C allows reducing cutting forces by 35 %. This evolution can be, partially, explained by the thermal softening got when the temperature increase. The steps described correspond to the evolution of mechanical properties as temperatures increasing. This evolution follows that of the material breaking limit and partially explains this trend [14].

3.2. Tool wear

Since the elevation of temperature during the hot machining process, it is important to explore the state of the insert. As shown Fig. 5, the tool wear mechanisms are different as a function of the heat. For the

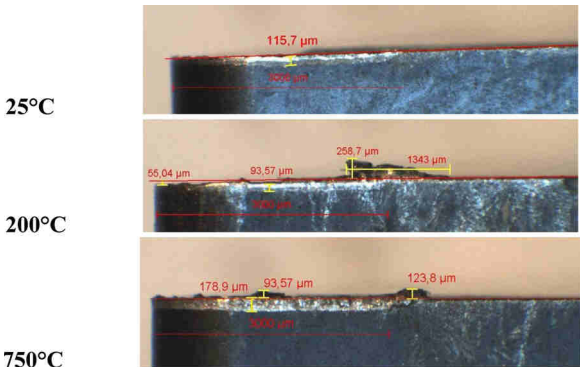

Fig. 5. Tool wear according to temperature.

test made at room temperature, a chipping occur near to the radial depth limit. This deterioration results from sever abrasion on rake face due to high pressures and titanium inclusions. These conclusions agree with the work of [14]. When the temperature increases, the tool wear mechanisms change. The new titanium alloys behaviour and the tribological aspects of the tool chip interface explain this evolution. Indeed, the increase of temperature modifies the titanium behaviour. When the temperature raises the Ti5553 is more ductile and therefore stickier. As we will see later, it is possible to correlate degradation modes and chip formation.

3.3. Chip formation

The workpiece temperature also modifies the chip morphology for several reasons. The first is the modification of material behaviour which induces a new chip formation. The second is the modification of the titanium microstructure. The initial temperature combined with the thermal energy generated by the cutting process and consequently the titanium cooling generate a new microstructure. Table 1exposes the chip microstructure for different cutting temperature. Firstly, it appears that regardless of the cutting temperature, the chips are always saw-tooth types. The shear angle is unchanged and the primary band frequency is never constant. Indeed, the chip analysis shows a stochastic distribution of the distance between each primary band. There is also the evolution of the primary shear bands thickness. The increase in temperature generates some largest shear bands. It should be noticed that for highest temperature the shear band thickness is not constant. As we will see later, very wide shear bands and extremely thin bands may appear. Consequently, the quantity of sheared titanium is strongly different.

Table 1
Chip morphology evolution.

T = 25 °C	T = 200 °C
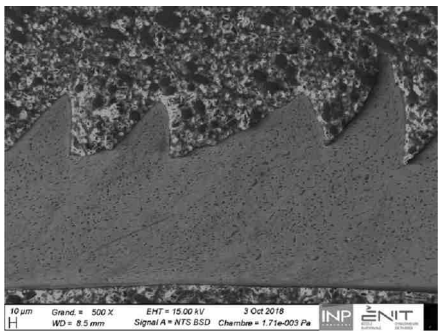	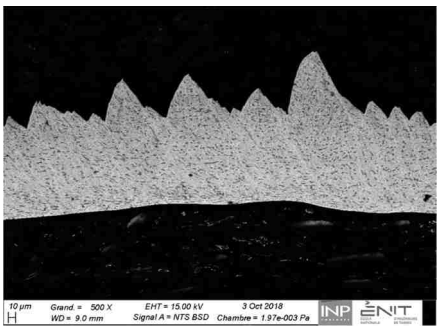
T = 400°C	T = 750°C
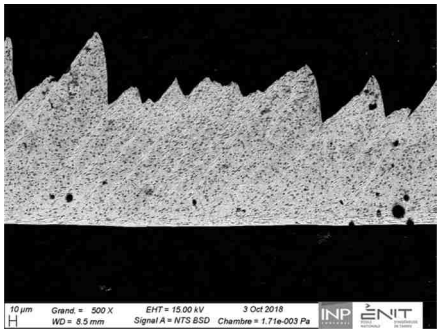	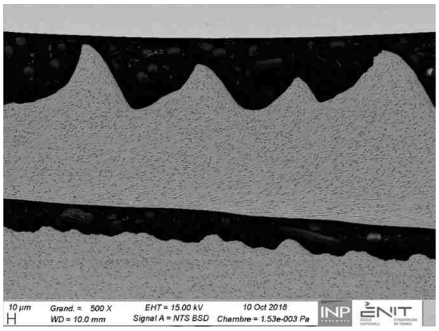

4. Chip formation simulation

To investigate the titanium alloy chip formation mechanism, a 3D thermomechanical finite element model was developed. However, the simulation of such complex process requires the mastery of many parameters: (i) materials behavior and chip formation criterion (ii) parts geometries, (iii) boundary conditions …

4.1. Initial geometry, meshes and boundary conditions

3D continuum elements under reduced integration (C3D8RT) were used for thermomechanical fields calculations. In particular, a mesh refinement was applied in the region of interest in order to improve the accuracy at the tool tip. Based on a mesh sensitivity analysis, the region of interest mesh size is set to 25 μm while the coarsest is between (200 − 500 μm). The workpiece is a parallelepiped part with a 1.8 mm in length, 0.35 mm in width and 0.75 mm in height. It is modelled by a single partition of favours the realistic material separation.

As Summarized in Fig. 6, the tool is fixed and the workpiece moves only along the X axis with a constant velocity (here 35 m.min-1).

4.2. Tool and workpiece behaviors

A classical thermo-elastic law was used to model the carbide tool behavior. Regarding the workpiece, a Johnson–Cook behavior model is adopted [15] (Eq. 1).

$$\sigma = [A+B(\varepsilon_p)^n]\left[1 + C\,\mathrm{Log}\left(\frac{\dot{\varepsilon}_p}{\dot{\varepsilon}_{p0}}\right)\right]\left[1 - \left(\frac{T-T_r}{T_m - T_r}\right)^m\right] \quad (1)$$

Where ε_p, $\dot{\varepsilon}_p$, $\dot{\varepsilon}_{p0}$ are respectively the plastic strain, the strain rate and reference plastic strain rate and T, T_r,T_m are the temperature, the room temperature, the melting temperature of the workpiece material. A, B, C, m, n are material parameters. The Johnson–Cook parameter for the Ti-555-3 titanium alloy are specified in Table 2, whereas the physical properties of both material are mentioned in Table 3.

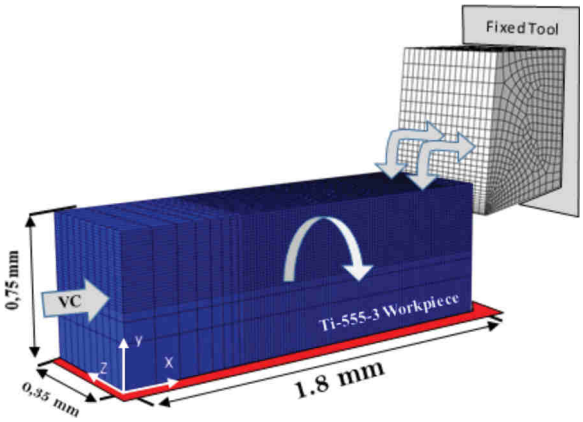

Fig. 6. 3D Orthogonal cutting FE model: Boundary condition and geometry.

Table 2
The Johnson-Cook behavior model parameters [16].

A (MPa)	B (MPa)	C	n	m	$\dot{\varepsilon}_{p0}$
1175	728	0.19	0.26	0.72	0.09

4.3. Damage criterion

Since the material failure mechanism in titanium alloy machining based on the ductile fracture, a specific damage model is developed through the coupling between the Johnson Cook flow behavior and the max shear stress criterion. The Max Shear (or Tresca) damage criterion can be expressed in terms of principal stresses by (Eq. 2):

$$\sigma_1 - \sigma_3 = 2\tau_f \quad (2)$$

However, the MS criteria can described and implemented though the equivalent strain at failure $\bar{\varepsilon}_f$. More details about the model

Table 3
Material and contact condition [14,16].

Materials	Property	Workpiece	Tool
	Density ρ (kg/m^3)	4650	15700
	Elastic modulus E (GPa)	112	705
	Poisson's ratio ϑ	0.32	0.23
	Specific heat C_p (J/kg°C)	[17]	178
	Thermal conductivity λ (W/m°C)	[17]	24
	Expansion coefficient $\alpha_{expansion}$ (μm/m/°C)	9	5
	Room temperature T_r (°C)	200-400-750	
	Inelastic heat fraction β_{TQ}	0.9	–
	Melting temperature Tm(°C)	1625	
Contact	Friction coefficient μ	0.2	
	Friction Energy transformed to heat	99 %	

transformation are described in [18]. Therefore, the MS damage criterion provides an expression of the equivalent strain at failure as a function of θ, τ_f, and the Johnson cook thermal and strain rate dependency terms:

$$\bar{\varepsilon_f} = \left[\frac{\sqrt{3}\,\tau_f}{B.\cos\left(\frac{\pi\theta}{6}\right)\left[1 + C\,Log\left(\frac{\dot{\varepsilon}_p}{\dot{\varepsilon}_{p0}}\right)\right]\left[1 - \left(\frac{T - T_r}{T_m - T_r}\right)^m\right]} - \frac{A}{B} \right]^{\frac{1}{n}} \quad (9)$$

The MS damage model requires only one parameter to be identified. This latter named maximum shear stress at failure τ_f. It is set to 1903 MPa [16]. The numerical chip morphology with temperature and the damage fields were respectively described in Figs. 7 and 8. Serrated chips generated from quasi-periodic cracks were observed for all simulations. In addition, a high level damage is identified between chips segments. It describes the thermo-mechanical loadings level and cracks propagations history provoked in machining.

Regarding the crack path, it starts at the tool tip and propagates within the material until achieves the material upper part. Such effect is observed by [19,20], during TA6V machining. In fact, this latter phenomenon is highly influenced by the heating temperature. More temperature is important and more crack propagation within the material decreases. Such effect resulting from the attenuation of strain rate effect by the heating of the part which induces the suppression of the competition between the thermal softening and the strain hardening. Consequently, the strain localisation becomes less important which leads to a reduced crack propagation.

Numerical cutting forces under different heating temperatures are depicted and compared to the experimental ones in Fig. 9. It should be mentioned that the cutting forces are highly influenced by the heating temperature. It decreases when the temperature increases. The numerical observations were validated by the experimental ones. However, the experimental forces present a small error for the simulation at 200 and 400 °C. Conversely, an error of 9,7 % is observed for the simulation at 750 °C. This error can be related to the friction behaviour model which not taken into account the temperature effect. After all, it can be said that the model predicts well the cutting forces and the chip morphology.

5. Discussion

Based on the simulation results, the chip observations and the microstructure, it is possible to explain the chip formation. For the room temperature, the mechanisms have been studied by [14]. This study exposes that the chip formation follows the mechanisms described by [21]. The chips collected are similar and consequently not studied in this article. However, when the temperature is modified, the alloy changes and new mechanisms occur.

When the temperature is 200 °C, the primary shear bands are very clear. They can be observed on focusing on α_p phases deformations. All of them are elongated in one orientation, the primary shear band, where a strong deformation of the grains is observed. The comparison between the initial form (circular) and the deformed one informs about the strain's value. Moreover, it should be noticed that the shear bands are very localised. The α_p nodules close to the shear bands stay totally circular and consequently not mechanically modified. The same observation can be made inside the bands where between α nodules deformed, the slate stay at their initial state. The β matrix is also affected because its size is bigger than the undeformed chip thickness (Fig. 13). In regarding the primary shear band, it occurs two behaviours. On the β matrix, concerning the α_s slate, the deformations are smallest compared to the α_p nodules. This difference can be explained by different points. Firstly, α_p is the softest phase above all compared to the β_{trans} phase [22]. After, the nature of the microstructure allows getting some dislocations. The dislocation from α phases to the β phases are facilitated by the Burger's relation. Contrary to them in the other way which is more difficult. The FEM results show that the temperatures are highest to β transus temperature. However, the EDX analysis doesn't reveal a real change of the titanium nature contrary to [14]. As with chips got at room temperature, it is possible to imagine that the shear strips are the result of an accumulation of high thermal stress and hardening. However, it can be assumed that their spread is facilitated by the presence of the α_p phases. Concerning the secondary shear zone, the results are quite different. Indeed, there are two areas. The first area near to the chip limit where occurs a microstructure totally homogeneous. As they move up towards the centre of the chip, alpha grains reappear. This microstructure is mainly due to the high temperature at the tool chip interface.

The formation of chips at 200 °C seems to correspond to the phenomena described by [23] and exposed in Fig. 13. When the tool penetrates into the material, a catastrophic shear failure occurs (Fig. 13b point (1)). At first, this phenomenon is parallel to the cutting speed orientation (Fig. 13 line 2) and then rises to the free surface of the chip (Fig. 13 line (3)), the connection between these two events is made by a radius of curvature. There is an intense deformation zone and a fracture zone at the tip of the chips indicating a crack. In the case of Ti5553, the intense deformation zone causes a very strong elongation of the nodular phases. A deformation pattern appears, facilitated by these elements. This difficult propagation is explained earlier in the paragraph. It

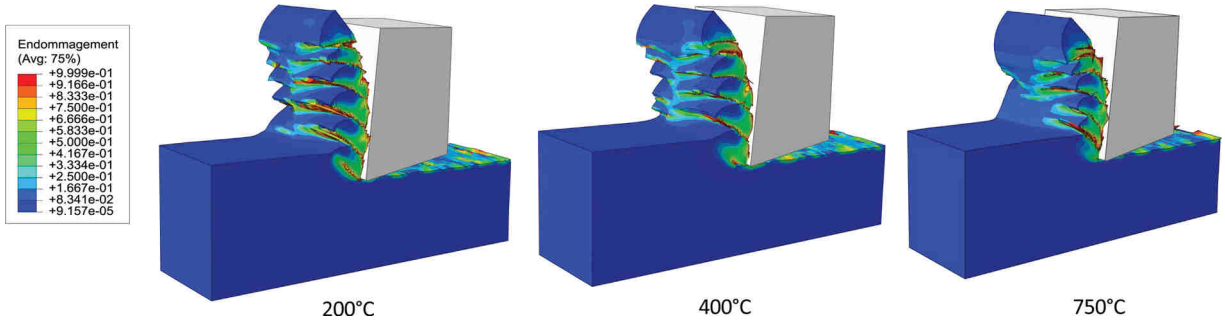

Fig. 7. 3D orthogonal cutting FE model – Damage.

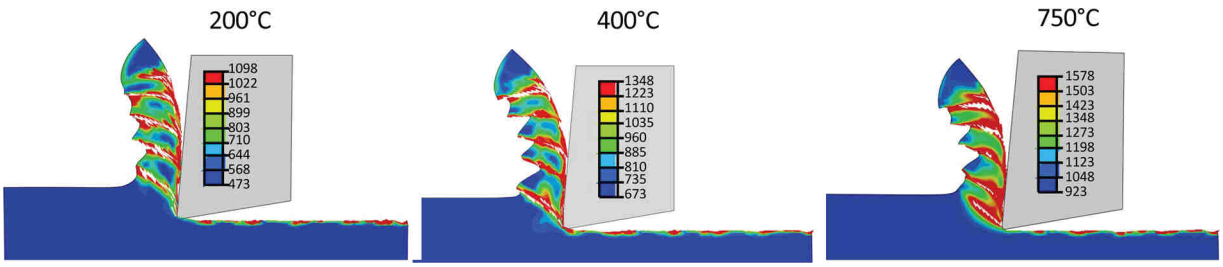

Fig. 8. 3D orthogonal cutting FE model - Temperature.

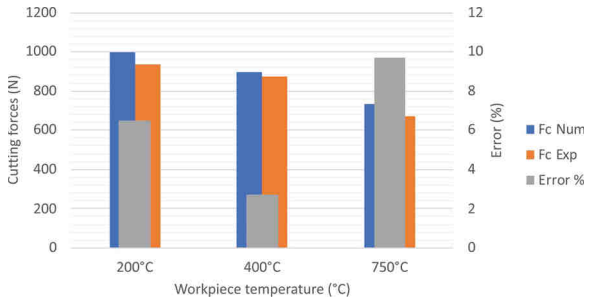

Fig. 9. Comparison between experimental and numerical cutting forces.

should be noticed that the temperature increases rapidly as explained by [24], however, the low thermal conductivity limits the effect on the microstructure and consequently in its evolution (Fig. 13b). The two close shear bands observed in some areas can be explained in two ways. The first is, as points out by [23], a deformation from the cutting edge through the free surface and a second in the opposite direction. The second explanation is a simultaneous propagation of two shear bands facilitated by an optimal α phase alignment from a dislocation point of view. Once this shear band is established, the material between the shear bands does not appear to be damaged. However, the ratio between the size of the ex-beta grains and the thickness of the chip suggests that it distorts the material. As temperature levels remain lower, the microstructure cannot be affected. This phenomenon has been studied by [25] where some EBSD analysis have been performed. When a saw-tooth chip is generated, intense pressure and temperature occur at the tool chip interface which induce high strain and large microstructure evolution (Fig. 13c). A new shear bands can be generated (Fig. 10).

The temperature increasing generates a new material where all the phases described in the previous sections are not visible. Fig. 11shows the microstructure in primary and secondary zone of a chip when T = 400 °C. As when T = 20 °C, the α grains are deformed along the same orientation. Between the primary and the secondary shear bands, the structure seems not changed. However, there is a crucial evolution. Indeed, the α_s slates disappear only in the primary shear bands. Although the phenomena occurring in the shear zones suggest that dynamic recrystallisation phenomena may occur. These first analysis shows a fraction of phase-free material whose nature depends greatly on the temperature generated. This evolution is due to the temperature [26]. The thickness of the primary shear bands is continuous compared to the previous test in despite of the softest material machined. It is explained by the homogenisation of the material where the behaviour difference between the phases is reduced. On the FEM model, the temperatures in these zones are higher than $T_{\beta transus}$ and suggest the microstructure evolution. For the secondary zone, its thickness increases, reflecting higher temperatures and pressures. α grains are also more elongated compared to the primary zone. The direction of

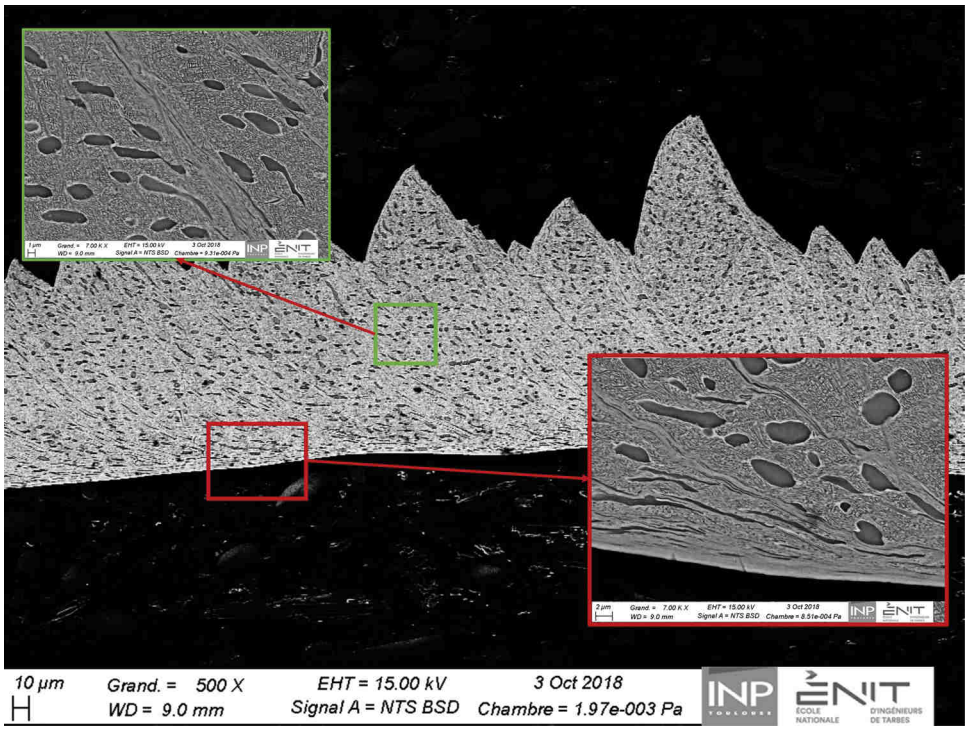

Fig. 10. Ti5553 microstructure when T = 200 °C.

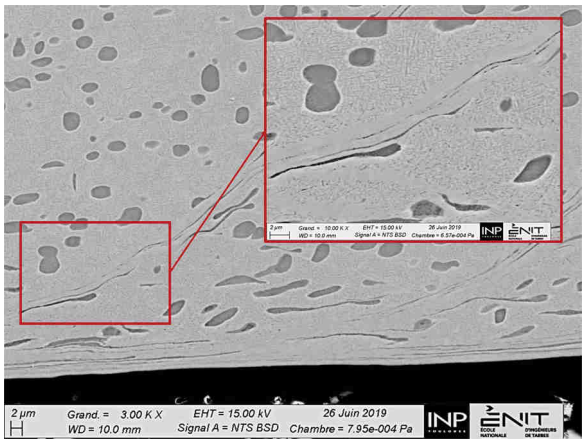

Fig. 11. Ti5553 miscrostrcture when T = 400 °C.

deformation is unique and parallel to the sliding speed of the chip on the cutting face.

For this temperature, the chip formation is conditioned by different factors which explained both the microstructure and the slight reduction in cutting forces. The phenomena involved during the initiation of the crack remain identical, as the initial microstructure does not seem to be modified (Fig. 13e). The difference is made when during the shear bands formation. Studies show that there is competition between hardening phenomena and thermal phenomena and that the shear band only appears when thermal effects become predominant. The latter are very localised and generate a very strong thermal softening. At this temperature, an additional phenomenon is present. The increase in temperature causes a microstructural modification where the α slates are completely dissolved. This phenomenon, as wide as the shear bands, favours the creation of these bands. The more homogeneous material promotes dislocations. This change in the nature of the alloy seems to be happening quickly (Fig. 13f). The cutting force reduction can also be explained by this chip formation. Indeed, this new microstructure facilitates the creation of shear bands (high thermal softening and initiation of dislocations facilitated) and therefore limits shear forces. As for the secondary zone, it is also totally devoid of α phase.

The chip formation and microstructure evolution are more significant when T = 750 °C. In general point of view, the morphology of the chips collected is not constant. For these conditions, there are two possibilities. The first is shown Fig. 1 where a sawtooth chip is generated. The main difference with the lower temperatures is some big primary shear bands. This chip formation follows the mechanisms exhibit previously. However, the thermal softening of the workpiece material requires a large volume of material to get the shear bands. The second possibility is exposed on Fig. 12. The slates observed in the β matrix have largely disappeared both in shear zones and in undeformed zones (Fig. 12). This evolution can also explain partially the cutting forces decrease. Indeed, the initial variable of the α phase, the alpha-grain boundary, the alphaWidmanstätten grain boundary and the morphology of the β phase can explain the low machinability of this titanium alloy [1]. Moreover [27] reveal the large decrease of the mechanical properties of the titanium when the temperature increase. Concerning the chip formation, the distance between shear strips appears to be less uniform as the chip and increase drastically.

At 750 °C, the phenomena are different because the microstructure is totally modified (Fig. 13g) before the chip formation. The absence of shear bands suggests that the phenomena involved are totally different. It would seem, given the thickness of the secondary zone, that the material is consequently cut. Indeed, there appears to be a very thick secondary. When the chip is separated from the part, a deformation propagates to the free surface of the chip. The latter is of low intensity because the α nodules are lightly deformed.

6. Limits of temperature increase

To define the advantage provide by the temperature increase, a power approach is used. Indeed, the definition of a sustainable assistance can be : the power used to help, in our case to increase the temperature, is lower than the power earning. Without considering the thermal dispersion (radius and convective effect), the power supplied to raise the temperature is defined (equation 6).

$$\phi = C_p M \frac{\delta T}{t}$$

where C_p is the heat capacity, M the sample weight, ∂T the temperature and ∂t the time to get the temperature. Fig. 14reveals the gain of power when the temperatures increase. Each blue line corresponds to the difference between the cutting power at the considered temperature and the cutting power when T = 20 °C. The orange lines are the power supplies to increase the temperature of the part. As seen on the Fig. 14, the power provides is always the lowest. Consequently and although the cutting force reduction is low, this help seems sustainable. However,

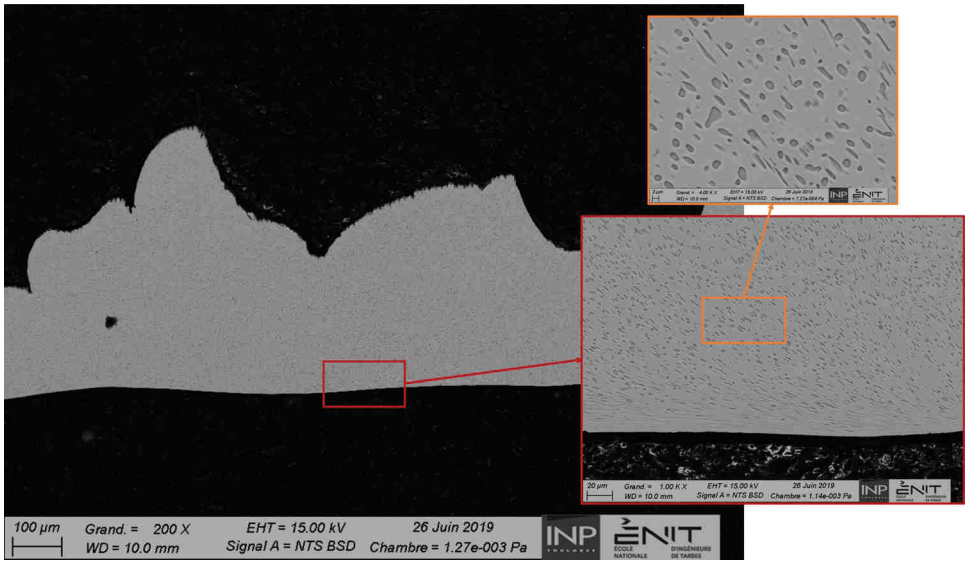

Fig. 12. Ti5553 microstructure when T = 750 °C.

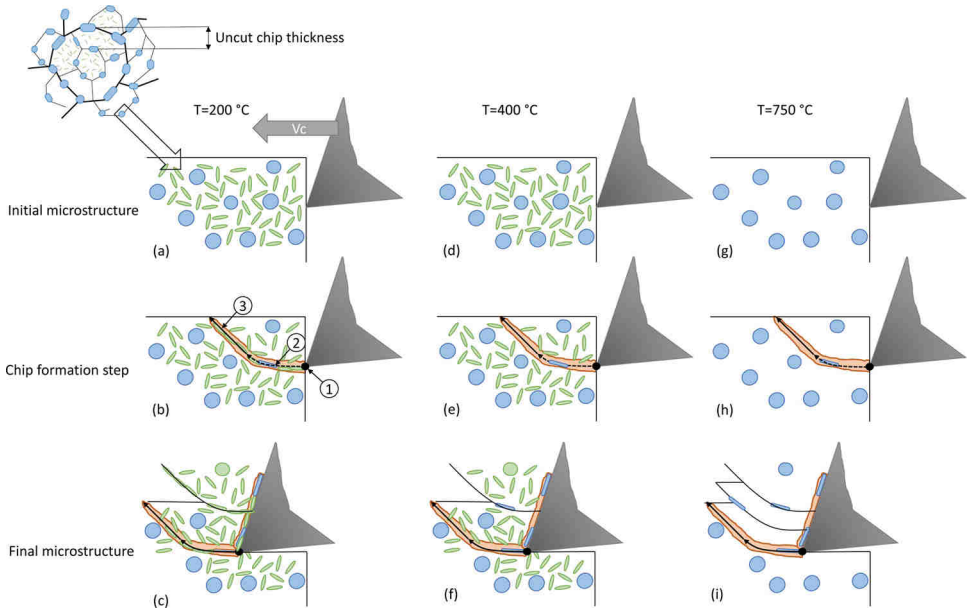

Fig. 13. Steps of the chip formation according to temperatures.

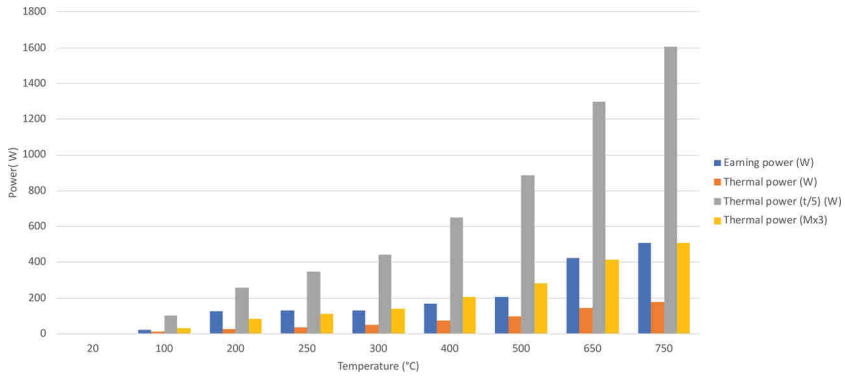

Fig. 14. Power gain and power provides to increase temperature.

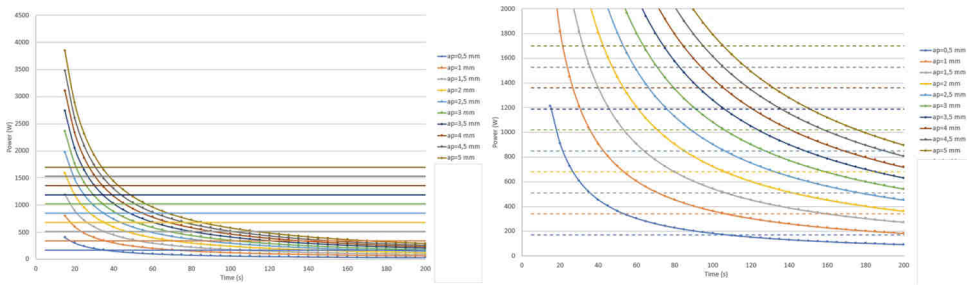

Fig. 15. Power gain and power provides to increase temperature.

the quantity of metal to heat is small or limited and the time is very long. If the part height is three times higher (yellow line), this assistance becomes not sustainable and the same conclusion is made when the time to increase the temperature is five times reduced.

The same approach has been applied on a turning operation. The thermal power corresponds to the power needs to increase the temperature of a tube which correspond to the volume of the material removed by the tool in a defined time. Contrary to the previous study, the heat source moves with the tool to heat a localized surface. The aim is to avoid to heat the entire part but only the a limited volume which can be removed in limiting the losses. For this study, the length is limited to L = 0,01 m. This power is defined equation 7:

$$\phi = C_p \rho L (R^2 - (R - a_p)^2) \pi \frac{\delta T}{t}$$

where R is the part radius (150 mm), ap is the radial depth, L the length of the heated tube (0,01 m) 750 °C.

As defined previously (Fig. 15), if the radial depth increases the power provided is larger (highest volume of material) and when the heating time increases the power reduces. To each radial depth, the dot lines correspond to the cutting power earning when T = 750 °C. When the time increases, the power needed becomes very large. Based on these figures, it occurs an interesting point. Indeed, the limit of a sustainable process is always defined when t = 180 s. This limits move

automatically when L is modified. For example, it moves to 20 s when L = 1 mm. In comparing the tool feed and the time to heat this limited length of material (without considering the convection and the radiation phenomenon), it seems very difficult to use this assistance only by focusing on the economic aspects during rough operations. Indeed, it is necessary to use more efficient heating means (to reduce the time to heat), therefore to the detriment of the economic gain and to combine these results with potentially significant gains in tool wear, for example.

7. Conclusion

Due to the difficulty of machining the Ti5553, many assistance systems have been tested. The hot machining technique seems to be a relevant solution. The principle is to heat the cutting zone and advantage from thermal softening. The objective of this work is to verify the relevance of this assistance on the machinability of Ti5553 and understand the phenomena involved. For this reason, an experimental device has been developed that allows temperature control over the whole depth of cut. The analysis shows that an increase in temperature does indeed lead to a reduction in cutting forces. This reduction seems to correlate with two aspects. The first is the reduction of mechanical properties with increasing temperature. The second is a different cutting process. From a wear point of view, although wear tests have not been carried out, totally different facies appear. Abrasive phenomena give way to an adherent chip. The increase in temperature leads to a different chip formation. At low temperatures (below 200 °C), shear bands appear as described in many works. Above 400 °C, a new phenomenon appears. The previously unchanged microstructure is now affected by the cutting process. This modification only occurs in the shear zones. For high temperatures, the cutting process is completely modified. The chip literally seems to have been cut. Lastly, a feasibility analysis shows that a purely economic consideration of this assistance shows a certain limit. The heating powers to be used for roughing operations become very important.

Declaration of Competing Interest

The authors report no declarations of interest.

References

[1] Arrazola P-J, Garay A, Iriarte L-M, Armendia M, Marya S, Le Maitre F. Machinability of titanium alloys (Ti6Al4V and Ti555. 3). J Mater Process Technol 2009;209(5):2223–30.

[2] Sun S, Brandt M, Dargusch MS. Thermally enhanced machining of hard-to-machine materials—a review. Int J Mach Tools Manuf 2010;50(8):663–80.

[3] Machado AR, Wallbank J, Pashby IR, Ezugwu EO. Tool performance and chip control when machining Ti6A14V and INCONEL 901 using high pressure coolant supply. Mach Sci Technol 1998;2(1):1–12.

[4] Braham-Bouchnak T, Germain G, Morel A, Furet B. Influence of high-pressure coolant assistance on the machinability of the titanium alloy Ti555–3. Mach Sci Technol 2015;19(1):134–51.

[5] Ayed Y, Germain G, Ben Salem W, Hamdi H. Experimental and numerical study of laser-assisted machining of Ti6Al4V titanium alloy. Finite Elem Anal Des 2014;92:72–9.

[6] Anderson M, Patwa R, Shin YC. Laser-assisted machining of Inconel 718 with an economic analysis. Int J Mach Tools Manuf 2006;46(14):1879–91.

[7] Komanduri R, Flom DG, Lee M. Highlights of the DARPA advanced machining research program. J Manuf Sci Eng 1985;107(4):325–35.

[8] Kaynak Armin Yilmaz UK. A comparison of flood cooling, minimum quantity lubrication and high pressure coolant on machining and surface integrity of titanium Ti-5553 alloy. J Manuf Process 2018;34:503–12.

[9] Thandra SK, Choudhury SK. Effect of cutting parameters on cutting force, surface finish and tool wear in hot machining. Int J Mach Mach Mater 2010;7(3–4).

[10] Macy JR. Heating device for hot machning apparatus. United States Pat Off 1995:304–928.

[11] Ginta T, Amin A, Lajis MA, Karim A, Radzi HCDM. Improved tool life in end milling Ti6Al4V through workpiece preheating. Eur J Sci Res 2009;27:384–91.

[12] Martin G. Numerical multiscale simulation of the mechanical behavior of beta-metastable titanium alloys Ti5553 and Ti17. Mines ParisTech 2012.

[13] ISO. ISO8688-1 – tool life testing in milling, part 1 : face milling. Int Organ Stand 1989. no. ISO8688-1.

[14] Wagner V, Baili M, Dessein G. The relationship between the cutting speed, tool wear, and chip formation during Ti-5553 dry cutting. Int J Adv Manuf Technol 2015;76(5–8):893–912.

[15] Ludwik P. Elemente der Technologischen Mechanik Elemente der Technologischen Mechanik. Springer; 1999.

[16] Braham Bouchnak T. Etude du comportement en sollicitations extrêmes et de l'usinabilité d'un nouvel alliage de titane aéronautique le TI555-3 2010.

[17] Wagner V. Amélioration de la productivité en usinage d'un titane refractaire : le Ti5553. Université de Toulouse; 2012.

[18] Harzallah M, Pottier T, Gilblas R, Landon Y, Mousseigne M, Senatore J. A coupled in-situ measurement of temperature and kinematic fields in Ti-6Al-4V serrated chip formation at micro-scale. Int J Mach Tools Manuf 2018;130–131:20–35.

[19] Pottier T, Germain G, Calamaz M, Morel A, Coupard D. Sub-millimeter measurement of finite strains at cutting tool tip vicinity. Exp Mech 2014;54(6):1031–42.

[20] Harzallah M. In-situ characterization and modelling of mechanisms and thermo-mechanical couplings in machining : application to Ti-6AL-4V titanium alloy. Ecole des Mines d'Albi-Carmaux 2018.

[21] Komanduri R, Von Turkovich BF. New observations on the mechanism of chip formation when machining titanium alloys. Wear 1981;69(2):179–88.

[22] Huang C, et al. High cycle fatigue behavior of Ti–5Al–5Mo–5V–3Cr–1Zr titanium alloy with bimodal microstructure. J Alloys Compd 2017;695:1966–75.

[23] Komanduri R, Hou Z-B. On thermoplastic shear instability in the machining of a titanium alloy (Ti-6Al-4V). Metall Mater Trans A 2002;33(9). p. 2995.

[24] Wagner V, et al. Comparison of the chip formations during turning of Ti64 β and Ti64 α + β. Proc Inst Mech Eng Part B J Eng Manuf 2017.

[25] Wagner V, Balcaen Y, Garnier C, Dessein GG, Alexi J. Etude de la formation des copeaux en tournage à sec du Ti5553. MUGV, Aubieres. 2014. France.

[26] Setterfati A. Experimental study and phase field modelling of alpha formation in near beta titanium alloys. Université de Lorraine; 2012.

[27] Warchomicka F, Poletti C, Stockinger M. Study of the hot deformation behaviour in Ti–5Al–5Mo–5V–3Cr–1Zr. Mater Sci Eng A 2011;528(28):8277–85.